Research article

Title

Spatial variations in terrestrial net ecosystem productivity and its local indicators

Running title

Spatial variability in terrestrial NEP

Authors

Erqian Cui[1,2] (eqcui@stu.ecnu.edu.cn)
Chenyu Bian[1,2] (cybian@stu.ecnu.edu.cn)
Yiqi Luo[3] (yiqi.luo@nau.edu)
Shuli Niu[4,5] (sniu@igsnrr.ac.cn)
Yingping Wang[6] (Yingping.Wang@csiro.au)
Jianyang Xia[1,2,*] (jyxia@des.ecnu.edu.cn)

Affiliations

[1]Zhejiang Tiantong Forest Ecosystem National Observation and Research Station, Shanghai Key Lab for Urban Ecological Processes and Eco-Restoration, School of Ecological and Environmental Sciences, East China Normal University, Shanghai 200241, China;
[2]Research Center for Global Change and Ecological Forecasting, East China Normal University, Shanghai 200241, China;
[3]Center for ecosystem science and society, Northern Arizona University, Arizona, Flagstaff, AZ 86011, USA.
[4]Key Laboratory of Ecosystem Network Observation and Modeling, Institute of Geographic Sciences and Natural Resources Research, Chinese Academy of Sciences, Beijing, China;
[5]University of Chinese Academy of Sciences, Beijing, China;
[6]CSIRO Oceans and Atmosphere, PMB 1, Aspendale, Victoria 3195, Australia.

Correspondence

Jianyang Xia, School of Ecological and Environmental Sciences, East China Normal University, Shanghai 200241, China.
Email: jyxia@des.ecnu.edu.cn

Key words

Net ecosystem productivity, spatial variation, CO_2 uptake and release, local indicators, model

Abstract

Multiple lines of evidence have demonstrated the persistence of global land carbon (C) sink during the past several decades. However, both annual net ecosystem productivity (NEP) and its inter-annual variation (IAV_{NEP}) keep varying over space. Thus, identifying local indicators for the spatially varying NEP and IAV_{NEP} is critical for locating the major and sustainable C sinks on the land. Here, based on daily NEP observations from FLUXNET sites and the atmospheric inversion product, we found a robust logarithmic correlation between annual NEP and ratio of total CO_2 exchanges during net uptake (U) and release (R) periods (i.e., U/R). The cross-site variation of mean annual NEP could be linearly indicated by $\ln(U/R)$, while the spatial distribution of IAV_{NEP} was well indicated by the slope (i.e., β) of the demonstrated logarithmic correlation. Among biomes, for example, forests and croplands had the largest U/R ratio (1.06 $\pm$ 0.83) and β (473 $\pm$ 112 g C m^{-2} yr^{-1}), indicating the highest NEP and IAV_{NEP} in forests and croplands, respectively. We further showed that these two simple indicators could directly infer the spatial variations in NEP and IAV_{NEP} in global gridded products. Overall, this study provides two simple local indicators for the intricate spatial variations in the strength and stability of land C sinks. These indicators could be helpful for locating the persistent terrestrial C sinks and provides valuable constraints for improving the simulation of land-atmospheric C exchanges.

1. Introduction

Terrestrial ecosystems reabsorb about one-quarter of anthropogenic CO_2 emission (Ciais et al., 2019) and are primarily responsible for the recent temporal fluctuations of the measured atmospheric CO_2 growth rate (Randerson, 2013; Le Quéré et al., 2018). In addition, evidence based on eddy-flux measurements (Baldocchi et al., 2018; Rödenbeck et al., 2018), aircraft atmospheric budgets (Peylin et al., 2013), and process-based model simulations (Poulter et al., 2014; Ahlstrom et al., 2015) has shown a large spatial variability in net ecosystem productivity (NEP) on the land. The elusive variation of terrestrial NEP over space refers to both of the substantial varying mean annual NEP and the divergent inter-annual variability (IAV) in NEP (i.e., IAV_{NEP}; usually quantified as the standard deviation of annual NEP) across space (Baldocchi et al., 2018; Marcolla et al., 2017). The mean annual NEP is related to the strength of carbon exchange of a specific ecosystem (Randerson et al., 2002; Luo and Weng, 2011; Jung et al., 2017), while IAV_{NEP} characterizes the stability of such carbon exchange (Musavi et al., 2017). Thus, whether and how NEP and IAV_{NEP} change over the space is important for predicting the future locations of carbon sinks on the land (Yu et al., 2014; Niu et al., 2017).

Large spatial difference in terrestrial NEP has been reported from eddy-flux measurements, model outputs and atmospheric inversion products. In addition, the global average IAV of NEP was large relative to global annual mean NEP (Baldocchi et al., 2018). More importantly, the spatial variations of NEP and IAV_{NEP} were typically underestimated by the compiled global product and the process-based global models (Jung et al., 2020; Fu et al., 2019). These discrepancies further revealed the necessary to identify local indicators for the spatially varying NEP and IAV_{NEP}, separately. The NEP in terrestrial ecosystems is determined by two components, including vegetation photosynthesis and ecosystem respiration (Reichstein et al., 2005). Because photosynthesis and respiration are strongly correlated over space (Baldocchi et al., 2015; Biederman et al., 2016), their relative difference could determine the spatial variation of NEP. Many previous analyses have attributed the IAV_{NEP} at the site level to the different sensitivities of ecosystem photosynthesis and respiration to environmental drivers (Gilmanov et al., 2005; Reichstein et al., 2005) and biotic controls (Besnard et al., 2018; Musavi et al., 2017). For example, some studies have reported that IAV_{NEP} is more associated with variations in

78 photosynthesis than carbon release (Ahlstrom et al., 2015; Novick et al., 2015; Li et al., 2017),
79 whereas others have indicated that respiration is more sensitive to anomalous climate variability
80 (Valentini et al., 2000; von Buttlar et al., 2017). However, despite the previous efforts in a
81 predictive understanding of the land-atmospheric C exchanges, the multi-model spread has not
82 reduced over time (Arora et al., 2019). Therefore, it is imperative to explore the potential
83 indicators for the spatially varying NEP, which could help attribute the spatial variation of NEP
84 and IAV_{NEP} into different processes and provide valuable constraints for the global C cycle.
85 Alternatively, the annual NEP of a given ecosystem can be also directly decomposed into CO_2
86 uptake flux and CO_2 release flux (Gray et al., 2014), which are more direct components for NEP
87 (Fu et al., 2019). Many studies have reported that the vegetation CO_2 uptake during the growing
88 season and the non-growing season soil respiration are tightly correlated (Luo et al., 2014; Zhao
89 et al., 2016). It is still unclear how the ecosystem CO_2 uptake and release fluxes would control
90 the spatially varying NEP.

91 Conceptually, the total CO_2 uptake flux (U) is determined by the length of CO_2 uptake
92 period (CUP) and the CO_2 uptake rate, while the total CO_2 release flux (R) depends on the length
93 of CO_2 release period (CRP) and the CO_2 release rate (Fig. 1b). The variations of NEP thus
94 should be innovatively attributed to these decomposed components. A strong spatial correlation
95 between mean annual NEP and length of CO_2 uptake period has been reported in evergreen
96 needle- and broad-leaved forests (Churkina et al., 2005; Richardson et al., 2013; Keenan et al.,
97 2014), whereas atmospheric inversion data and vegetation photosynthesis model indicated a
98 dominant role of the maximal carbon uptake rate (Fu et al., 2017; Zhou et al., 2017). However,
99 the relative importance of these phenological and physiological indicators for the spatially
100 varying NEP remains unclear.

101 In this study, we decomposed annual NEP into U and R, and explored the local indicators
102 for spatially varying NEP. Based on the eddy-covariance fluxes from FLUXNET2015 Dataset
103 (Pastorello et al., 2017) and the atmospheric inversion product (Rödenbeck et al., 2018), we
104 examined the relationship between NEP and its direct components. In addition, we used the
105 observations to evaluate the spatial variations of NEP and IAV_{NEP} in the FLUXCOM product
106 and a process-based model (CLM4.5) (Oleson et al., 2013). The major aim of this study is to

explore whether there are useful local indicators for the spatially varying NEP and IAV_{NEP} in terrestrial ecosystems.

2. Materials and Methods

2.1 Datasets

Daily NEP observations of eddy covariance sites are obtained from the FLUXNET2015 Tier 1 dataset (http://fluxnet.fluxdata.org/data/fluxnet2015-dataset/). The FLUXNET2015 dataset provides half-hourly data of carbon, water and energy fluxes at over 210 sites that are standardized and gap-filled (Pastorello et al., 2017). However, time series of most sites are still too short for the analysis of inter-annual variation in NEP. So only the sites that provided the availability of eddy covariance flux measurements for at least 5 years are selected. This leads to a global dataset of 72 sites with different biomes across different climatic regions. Based on the biome classification from the International Geosphere-Biosphere Programme (IGBP) provided for the FLUXNET2015 sites, the selected sites include 35 forests (FOR), 15 grasslands (GRA), 11 croplands (CRO), 4 wetlands (WET), 2 shrublands (SHR) and 5 savannas (SAV) (Fig. S1 and Table S1).

The Jena CarboScope Inversion product compiles from high precision measurements of atmospheric CO_2 concentration with simulated atmospheric transport (Rödenbeck et al., 2018). Here, we used the daily land-atmosphere CO_2 fluxes from the s85_v4.1 version at a spatial resolution of 5°× 3.75°. Considering the relatively low spatial resolution of the Jena Inversion product, the daily fluxes were only used to calculate the local indicators for the spatially varying NEP at the global scale.

Daily NEP simulations from Community Land Model version 4.5 (CLM4.5) were also used to calculate the local indicators for the spatially varying NEP at the corresponding flux tower sites. We ran the CLM4.5 model from 1985 to 2010 at a spatial resolution of 1° with CRUNECP meteorological forcing. Here, NEP was derived as the difference between GPP and TER, and TER was calculated as the sum of simulated autotrophic and heterotrophic respiration. The daily outputs from CLM4.5 were used to calculate the local indicators for the spatially varying NEP both at the global scale and at the FLUXNET site level.

The FLUXCOM product presents an upscaling of carbon flux estimates from 224 flux tower sites based on multiple machine learning algorithms and meteorological drivers (Jung et al., 2017). To be consistent with the meteorological forcing of Jena Inversion product and the CLM4.5 model, we used the FLUXCOM CRUNCEPv6 products. In addition, in order to reduce the uncertainty caused by machine-learning methods, we averaged all the FLUXCOM CRUNCEPv6 products with different machine-learning methods. It should be noted that the inter-annual variability of FLUXCOM product is only driven by climatic conditions, the effects of land use and land cover change are not represented. The FLUXCOM NEP product is downloaded from the Data Portal of the Max Planck Institute for Biochemistry (https://www.bgc-jena.mpg.de). Daily outputs from FLUXCOM for the period 1985-2010 at 0.5° spatial resolution were used to calculate the local indicators for the spatially varying NEP both at the global scale and at the FLUXNET site level.

2.2 Decomposition of NEP and the calculations for its local indicators

The annual NEP of a given ecosystem can be defined numerically as the difference between the CO_2 uptake and release. As illustrated in Figure 2b:

$$NEP = U - R \quad (1)$$

These components of NEP contain both photosynthesis and respiration flux, which directly indicate the net CO_2 exchange of an ecosystem. The total CO_2 uptake flux (U) and the total CO_2 release flux (R) can be further decomposed as:

$$U = \overline{U} \times CUP \quad (2)$$

$$R = \overline{R} \times CRP \quad (3)$$

where the $\overline{U}$ (g C m^{-2} d^{-1}) is the mean daily CO_2 uptake over CUP (d yr^{-1}) and $\overline{R}$ (g C m^{-2} d^{-1}) represents the mean daily CO_2 release over CRP (d yr^{-1}). In addition, we further tested the relationship between annual NEP and the ratio of $\frac{U}{R}$ (i.e., $NEP \propto \frac{U}{R}$). Ecologically, the ratio of $\frac{U}{R}$ reflects the relative strength of the ecosystem CO_2 uptake. Therefore, NEP in any year of any given ecosystem can be expressed as:

$$NEP = \beta \cdot \ln\left(\frac{U}{R}\right) \quad (4)$$

where the parameter β represents the slope of the linear relationship of $NEP \propto \ln\left(\frac{U}{R}\right)$. Based on the definitions of U and R, the ratio $\frac{U}{R}$ can be further written as:

$$\frac{U}{R} = \frac{\overline{U}}{\overline{R}} \cdot \frac{CUP}{CRP} \quad (5)$$

Ecologically, the ratio of $\frac{\overline{U}}{\overline{R}}$ reflects the relative physiological difference between ecosystem CO_2 uptake and release strength, while the ratio of $\frac{CUP}{CRP}$ is an indicator of net ecosystem CO_2 exchange phenology. Environmental changes may regulate these ecological processes and ultimately affect the ecosystem NEP. The slope β indicates the response sensitivity of NEP to the changes in phenology and physiological processes. All of β, $\frac{CUP}{CRP}$ and $\frac{\overline{U}}{\overline{R}}$ were then calculated from the selected eddy covariance sites and the corresponding pixels of these sites in models. These derived indicators from eddy covariance sites were then used to benchmark the results extracted from the same locations in models.

2.4 Calculation of the relative contributions

We further quantified the relative contributions of $\frac{\overline{U}}{\overline{R}}$ and $\frac{CUP}{CRP}$ in driving the spatial variations in NEP:

$$\mathrm{NEP} = \int\left(\frac{\overline{U}}{\overline{R}}, \frac{CUP}{CRP}\right) \quad (6)$$

We used a relative importance analysis method to quantify the relative contributions of each ratio to the spatial variations in NEP. The algorithm was performed with the "ralaimpo" package in R (R Development Core Team, 2011). The "relaimpo" package is based on variance decomposition for multiple linear regression models. We chose the most commonly used method named "Lindeman-Merenda-Gold (LMG)" (Grömping, 2007) from the methods provided by the "ralaimpo" package. This method allows us to quantify the contributions of explanatory variables in a multiple linear regression model. Across the 72 FLUXNET sites, we quantified the relative importance of $\frac{\overline{U}}{\overline{R}}$ and $\frac{CUP}{CRP}$ to cross-site changes in NEP.

185 **3. Results**

186 **3.1 The relationship between NEP and its direct components**

187 To find local indicators for the spatially varying NEP in terrestrial ecosystems, we tested the
188 relationship between NEP and its direct components (U and R) across the 72 flux-tower sites.
189 The results showed that annual NEP was closely related with the ratio of $\frac{U}{R}$ (Fig. S2). The
190 logarithmic correlations between annual NEP and $\frac{U}{R}$ were significant at all sites (Fig. 1a), and
191 ~90% of R^2 falling within a range from 0.7 to 1 (Fig. 1c).

192 In addition, the relationship between NEP and $\frac{U}{R}$ was also verified by the atmospheric
193 inversion product (i.e., Jena CarboScope Inversion). The control of $\frac{U}{R}$ on annual NEP was
194 robust in most global grid cells (i.e. $0.6 < R^2 < 1$). The explanation of $\frac{U}{R}$ was higher in 80% of
195 the regions, but lower in North American (Fig. 2). These two datasets both showed that the
196 indicator $\frac{U}{R}$ could successfully capture the variability in annual NEP.

197 **3.2 Local indicators for spatially varying NEP**

198 Across the 72 flux-tower sites, the spatial changes in mean annual NEP were significantly
199 correlated to $\ln(\frac{U}{R})$ ($R^2 = 0.65$, $P < 0.01$) (Fig. 3a). This finding suggested that the mean annual
200 ratio $\ln(\frac{U}{R})$ is a good indicator for cross-site variation in NEP. By contrast, the spatial variation
201 of IAV_{NEP} was moderately explained by the slope (i.e., β) of the temporal correlation between
202 NEP and $\ln(\frac{U}{R})$ at each site ($R^2 = 0.39$, $P < 0.01$; Fig. 3b) rather than $\ln(\frac{U}{R})$ (Fig. S3). The
203 wide range of ratio β reveals a large divergence of NEP sensitivity across biomes, ranging from
204 121 ± 118 g C m^{-2} yr^{-1} in shrubland to 473 ± 112 g C m^{-2} yr^{-1} in cropland.

205 The decomposition of indicator $\frac{U}{R}$ into $\frac{\bar{U}}{\bar{R}}$ and $\frac{CUP}{CRP}$ allowed us to quantify the relative
206 importance of these two ratios in driving NEP variability. The linear regression and relative
207 importance analysis showed a more important role of $\frac{CUP}{CRP}$ (58%) than $\frac{\bar{U}}{\bar{R}}$ (42%) in explaining
208 the cross-site variation of NEP (Fig. 4). Therefore, the spatial distribution of mean annual NEP

was mostly driven by the phenological rather than physiological changes.

3.3 Simulated spatial variations in NEP by models

We further used these two simple indicators (i.e., $\frac{U}{R}$ and β) to evaluate the simulated spatial variations of NEP by the compiled global product (i.e., FLUXCOM) and a widely-used process-based model at the FLUXNET site level (i.e., CLM4.5). We found that the low spatial variation of mean annual NEP in FLUXCOM and CLM4.5 could be inferred from their more converging $\ln(\frac{U}{R})$ than flux-tower measurements (Fig. 5). The underestimated variation of IAV_{NEP} in these modeling results was also clearly shown by the smaller β values (268.22, 126.00 and 145.08 for FLUXNET, FLUXCOM and CLM4.5, respectively) (Fig. 5b).

In addition, the spatial variations of NEP and IAV_{NEP} were associated with the spatial resolution of the product (Marcolla et al., 2017). Considering the scale mismatch between FLUXNET sites and the gridded product, we run the same analysis at the global scale based on Jena Inversion product. At the global scale, the spatial variation of mean annual NEP can be also well indicated by $\ln(\frac{U}{R})$ (Fig. 6). The larger C uptake in FLUXCOM resulted from its higher simulations for $\ln(\frac{U}{R})$. Furthermore, the larger spatial variation of IAV_{NEP} in CLM4.5 could be inferred from the indicator β.

4. Discussion

4.1 New perspective for locating the major and sustainable land C sinks

Large spatial differences of mean annual NEP and IAV_{NEP} have been well-documented in previous studies (Jung et al., 2017; Marcolla et al., 2017; Fu et al., 2019). Here we provide a new perspective for quantifying the spatially varying NEP by tracing annual NEP into several local indicators. Therefore, these traceable indicators could provide useful constraints for predicting annual NEP, especially in areas without eddy-covariance towers.

Typically, the C sink capacity and its stability of a specific ecosystem are characterized separately (Keenan et al., 2014; Ahlstrom et al., 2015; Jung et al., 2017). Here we integrated NEP into two simple indicators that could directly locate the major and sustainable land C sink.

Among biomes, forests and croplands had the largest $\ln(\frac{U}{R})$ and β, indicating the strongest and the most unstable C sink in forests and croplands, respectively. However, the relatively lower β in shrublands and savannas should be interpreted cautiously. There are very few semi-arid ecosystems in the FLUXNET sites, while they represent a large portion of land at the global scale and have been shown to substantially control the interannual variability of NEP (Ahlström et al., 2015). The highest β in croplands implies that the rapid global expansion of cropland may enlarge the IAV_{NEP} on the land. In fact, the cropland expansion has been confirmed as one important driver of the recent increasing global vegetation growth peak (Huang et al., 2018) and atmospheric CO_2 seasonal amplitude (Gary et al., 2014; Zeng et al., 2014).

4.2 Phenology-dominant spatial distribution of mean annual NEP

Recent studies have demonstrated that the spatiotemporal variations in terrestrial gross primary productivity are jointly controlled by plant phenology and physiology (Xia et al., 2015; Zhou et al., 2016). Here we demonstrated the dominant role of the phenology indicator $\frac{CUP}{CRP}$ in driving the spatial difference of mean annual NEP. The reported low correlation between mean annual NEP and the physiological indicator $\frac{\bar{U}}{\bar{R}}$ could partly be attributed to the convergence of $\frac{\bar{U}}{\bar{R}}$ across FLUXNET sites (Fig. S4).

The convergent $\frac{\bar{U}}{\bar{R}}$ across sites was first discovered by Churkina *et al*. (2005) as 2.73 ± 1.08 across 28 sites, which included DBF, EBF and crop/grass. In this study, we found the $\frac{\bar{U}}{\bar{R}}$ across the 72 sites is 2.71 ± 1.61, which validates the discovery by Churkina *et al*. However, the $\frac{\bar{U}}{\bar{R}}$ varied among biomes (2.86 ± 1.56 for forest, 2.16 ± 1.14 for grassland, 3.47 ± 1.98 for cropland, 2.89 ± 1.47 for wetland, 1.89 ± 1.10 for shrub, 1.83 ± 0.88 for savanna). This spatial convergence of $\frac{\bar{U}}{\bar{R}}$ at the ecosystem level provides important constraints for global models that simulate various physiological processes (Peng et al., 2015; Xia et al., 2017). These findings imply that the phenology changes will greatly affect the locations of the terrestrial carbon sink by modifying the length of carbon uptake period (Richardson et al., 2013; Keenan et al., 2014).

4.3 The simulated local indicators from gridded products

This study showed that the considerable spatial variations in mean annual NEP and IAV_{NEP} from global gridded products could also be inferred from their local indicators. The low variations of $\frac{U}{R}$ ratio in CLM4.5 could be largely due to their simple representations of the diverse terrestrial plant communities into a few plant functional types with parameterized properties (Cui et al., 2019; Sakschewski et al., 2015). In addition, the higher $\frac{U}{R}$ ratio from FLUXCOM product indicated its widely reported larger C uptake (Fig. 6) (Jung et al., 2020). Meanwhile, the ignorance of fire, land-use change and other disturbances could lead to the smaller β by allowing for only limited variations of phenological and physiological dynamics (Reichstein et al., 2014; Kunstler et al., 2016). Although the magnitude of IAV_{NEP} depends on the spatial resolution (Marcolla et al., 2017), we recommend future model benchmarking analyses to use not only the global product compiled from machine-learning method (Bonan et al., 2018) but also the site-level measurements or indicators (i.e., $\ln(\frac{U}{R})$ and β).

4.4 Conclusions and further implications

In summary, this study highlights the changes in NEP and IAV_{NEP} over space on the land, and provides the $\frac{U}{R}$ ratio and β as two simple local indicators for their spatial variations. These indicators could be helpful for locating the persistent terrestrial C sinks in where the $\ln(\frac{U}{R})$ ratio is high but the β is low. Their estimates based on observations are also valuable for benchmarking and improving the simulation of land-atmospheric C exchanges in Earth system models.

In addition, the findings in this study have some important implications for understanding the variation of NEP on the land. First, forest ecosystems have the largest annual NEP due to the largest $\ln(\frac{U}{R})$ while croplands show the highest IAV_{NEP} because of the highest β. Second, the spatial convergence of $\frac{\overline{U}}{\overline{R}}$ suggests a tight linkage between plant growth and the non-growing season soil microbial activities (Xia et al., 2014; Zhao et al., 2016). However, it remains unclear whether the inter-biome variation in $\frac{\overline{U}}{\overline{R}}$ is due to different plant-microbe interactions between biomes. Third, the within-site convergent but spatially varying β needs better understanding.

Previous studies have shown that a rising standard deviation of ecosystem functions could indicate an impending ecological state transition (Carpenter and Brock, 2006; Scheffer et al., 2009). Thus, a sudden shift of the β-value may be an important early-warning signal for the critical transition of IAV_{NEP} of an ecosystem. Furthermore, considering the limited eddy-covariance sites with long-term observations, these findings need further validation once the longer time-series of measurements from more sites and vegetation types become available.

Acknowledgements

This work was financially supported by the National Key R&D Program of China (2017YFA0604600), National Natural Science Foundation of China (31722009, 41630528) and National 1000 Young Talents Program of China. This work used eddy covariance dataset acquired and shared by the FLUXNET community, including these networks: AmeriFlux, AfriFlux, AsiaFlux, CarboAfrica, CarboEuropeIP, CarboItaly, CarboMont, ChinaFlux, Fluxnet-Canada, GreenGrass, ICOS, KoFlux, LBA, NECC, OzFlux-TERN, TCOS-Siberia, and USCCC. The ERA-Interim reanalysis data are provided by ECMWF and processed by LSCE. The FLUXNET eddy covariance data processing and harmonization was carried out by the European Fluxes Database Cluster, AmeriFlux Management Project, and Fluxdata project of FLUXNET, with the support of CDIAC and ICOS Ecosystem Thematic Center, and the OzFlux, ChinaFlux and AsiaFlux offices.

Data availability statement. Eddy flux data are available at http://fluxnet.fluxdata.org/data/fluxnet2015-dataset/**;** the data supporting the findings of this study are available within the article and the Supplementary Information.

Author contribution. E. Cui and J. Xia devised and conducted the analysis. Y. Luo, S. Niu, Y. Wang and C. Bian provided critical feedback on the method and results. All authors contributed to discussion of results and writing the paper.

Competing interests. The authors declare that there is no conflict of interest.

FIGURES

Figure 1 Relationship between annual NEP and $\frac{U}{R}$ for 72 FLUXNET sites (of the form $\mathrm{NEP} = \beta \cdot \ln(\frac{U}{R})$). a, Dependence of annual NEP on the ratio between total CO_2 exchanges during net uptake (U) and release (R) periods (i.e., $\frac{U}{R}$). Each line represents one flux site with at least 5 years of observations. b, Conceptual figure for the decomposition framework introduced in this study. Annual NEP can be quantitatively decomposed into the following indicators: $NEP = U - R$. c, Distribution of the explanation of $\frac{U}{R}$ on temporal variability of NEP (R^2) for FLUXNET sites.

Figure 2 Relationship between annual NEP and $\frac{U}{R}$ for Jena Inversion product (of the form $\mathrm{NEP} = \beta \cdot \ln(\frac{U}{R})$). The black box indicates the location of the sample.

Figure 3 Contributions of the two indicators in explaining the spatial patterns of mean annual NEP and IAV_{NEP}. a, The relationship between annual mean NEP and $\ln(\frac{U}{R})$ across FLUXNET sites (R^2 = 0.65, P < 0.01). The insets show the variation of $\ln(\frac{U}{R})$ for different terrestrial biomes. b, The explanation of β on IAV_{NEP} (R^2 = 0.39, P < 0.01). The insets show the distribution of parameter β for different terrestrial biomes. The number of site-years at each site is indicated with the size of the point.

Figure 4 The linear regression between $\frac{U}{R}$ with $\frac{CUP}{CRP}$ (R^2 = 0.71, P < 0.01) and $\frac{\bar{U}}{\bar{R}}$ (R^2 = 0.09, P < 0.01) across sites. The insets show the relative contributions of each indicator to the spatial variation of $\frac{U}{R}$. The number of site-years at each site is indicated with the size of the point.

Figure 5 Representations of the spatially varying NEP and its local indicators in FLUXCOM product and the Community Land Model (CLM4.5) at the FLUXNET site level. a, The variation of mean annual NEP and IAV_{NEP} derives from FLUXNET, FLUXCOM and CLM4.5. Variation in mean annual NEP: the standard deviation of mean annual NEP across sites; Variation in IAV_{NEP}: the standard deviation of IAV_{NEP} across sites. b, Representations of the local indicators for NEP in FLUXNET, FLUXCOM and CLM4.5. The corresponding distributions of $\ln\left(\frac{U}{R}\right)$ and β are shown at the top and right. Significance of the relationship between annual NEP and

338 $\ln\left(\frac{U}{R}\right)$ for each site is indicated by the circle: closed circles: $P<0.05$; open circles: $P>0.05$. Note
339 that the modeled results are from the pixels extracted from the same locations of the flux tower
340 sites.

341 **Figure 6** Representations of the spatially varying NEP and its local indicators in FLUXCOM
342 product and the Community Land Model (CLM4.5) at the global scale. a, The variation of mean
343 annual NEP and IAV_{NEP} derives from Jena Inversion, FLUXCOM and CLM4.5. Variation in
344 mean annual NEP: the spatial variation of mean annual NEP; Variation in IAV_{NEP}: the spatial
345 variation of standard deviation in IAV_{NEP}. b, Representations of the local indicators for NEP in
346 Jena Inversion, FLUXCOM and CLM4.5.
347

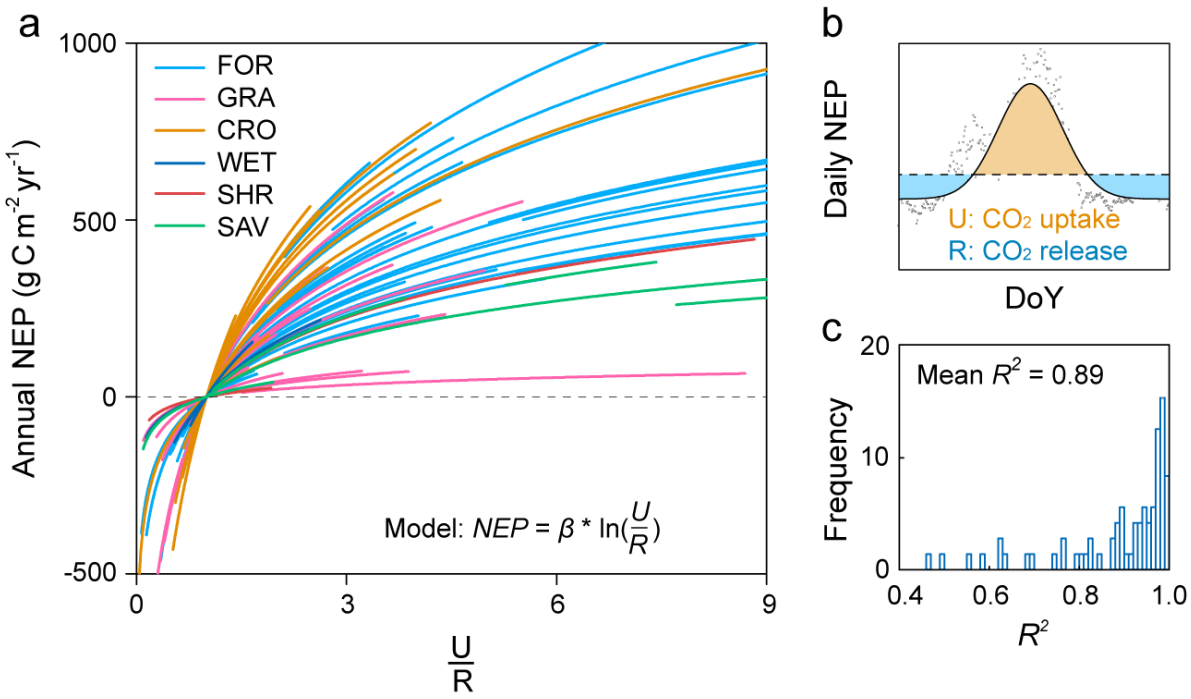

348

349 **Figure 1** Relationship between annual NEP and $\frac{U}{R}$ for 72 FLUXNET sites (of the form NEP =

350 $\beta \cdot \ln(\frac{U}{R})$). **a**, Dependence of annual NEP on the ratio between total CO_2 exchanges during net

351 uptake (U) and release (R) periods (i.e., $\frac{U}{R}$). Each line represents one flux site with at least 5

352 years of data. **b**, Conceptual figure for the decomposition framework introduced in this study.

353 Annual NEP can be quantitatively decomposed into the following indicators: $NEP = U - R$. **c**,

354 Distribution of the explanation of $\frac{U}{R}$ on temporal variability of FLUXNET NEP (R^2) for

355 FLUXNET sites.

356

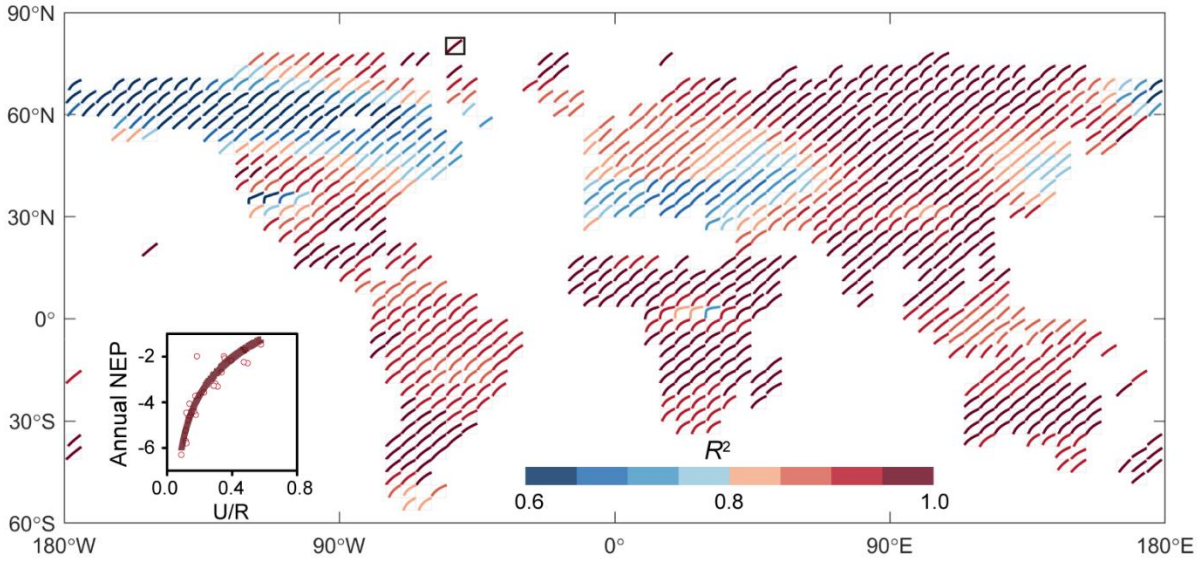

357

358 **Figure 2** Relationship between annual NEP and $\frac{U}{R}$ for Jena Inversion product (of the form

359 $\mathrm{NEP} = \beta \cdot \ln(\frac{U}{R})$). The black box indicates the location of the sample.

360

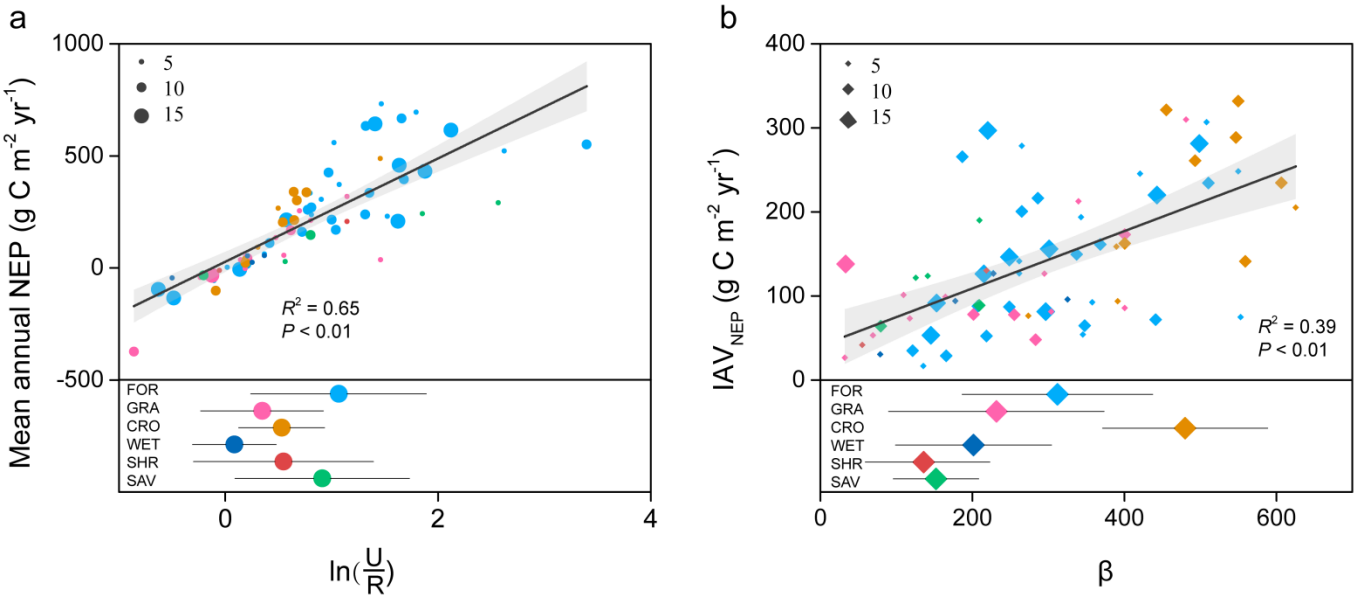

361

362 **Figure 3** Contributions of the two indicators in explaining the spatial patterns of mean annual

363 NEP and IAV_{NEP}. **a**, The relationship between annual mean NEP and $\ln(\frac{U}{R})$ across FLUXNET

364 sites (R^2 = 0.65, P < 0.01). The insets show the variation of $\ln(\frac{U}{R})$ for different terrestrial

365 biomes. **b**, The explanation of β on IAV_{NEP} ($R^2 = 0.39$, $P < 0.01$). The insets show the distribution

366 of parameter β for different terrestrial biomes. The number of site-years at each site is indicated

367 with the size of the point.

368

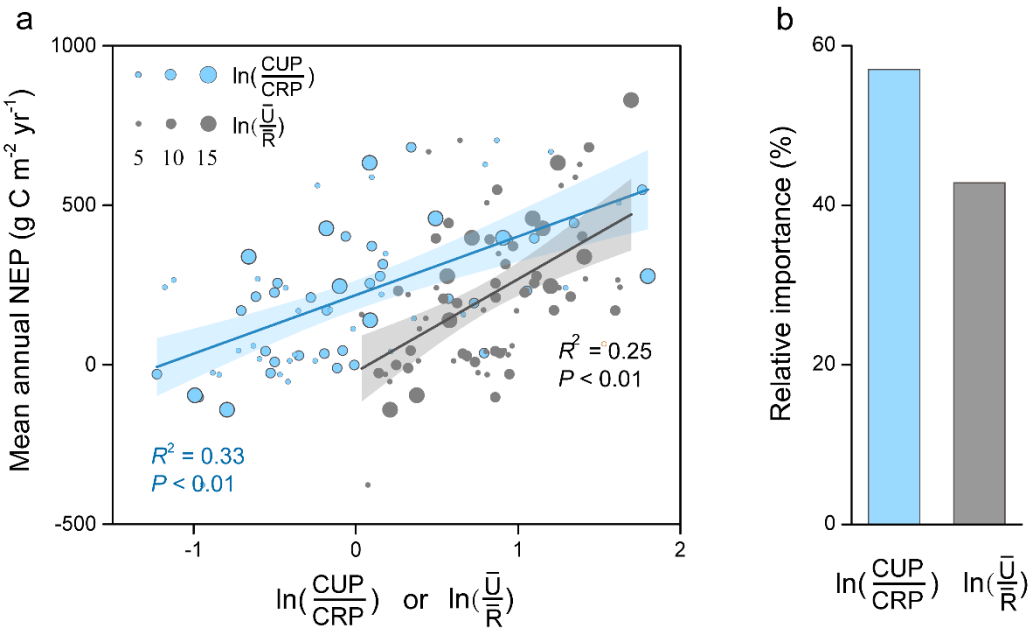

Figure 4 The relative contributions of the local indicators in explaining the spatial patterns of mean annual NEP. **a**, The linear regression between mean annual NEP with $\frac{CUP}{CRP}$ (R^2 = 0.33, P < 0.01) and $\frac{\bar{U}}{\bar{R}}$ (R^2 = 0.25, P < 0.01) across sites. **b**, The relative contributions of each indicator to the spatial variation of NEP. The number of site-years at each site is indicated with the size of the point.

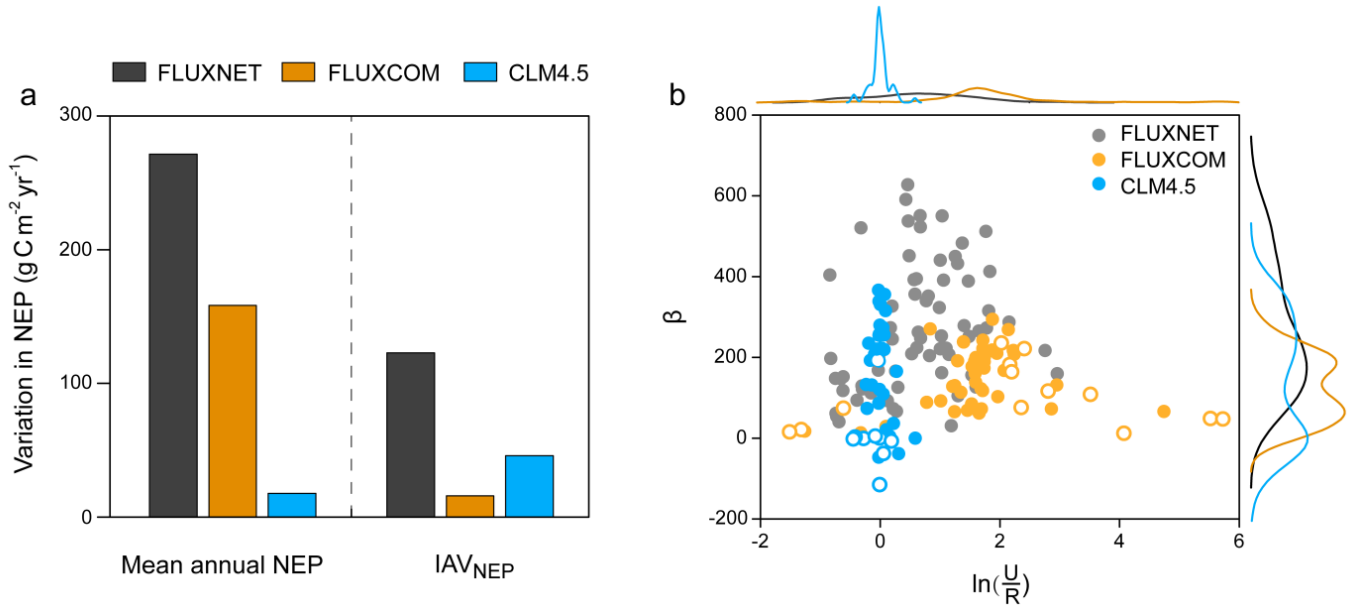

376

377 **Figure 5** Representations of the spatially varying NEP and its local indicators in FLUXCOM
378 product and the Community Land Model (CLM4.5) at the FLUXNET site level. **a**, The variation
379 of mean annual NEP and IAV_{NEP} derives from FLUXNET, FLUXCOM and CLM4.5. Variation
380 in mean annual NEP: the standard deviation of mean annual NEP across sites; Variation in
381 IAV_{NEP}: the standard deviation of IAV_{NEP} across sites. **b**, Representations of the local indicators
382 for NEP in FLUXNET, FLUXCOM and CLM4.5. The corresponding distributions of $\ln\left(\frac{U}{R}\right)$
383 and β are shown at the top and right. Significance of the relationship between annual NEP and
384 $\ln\left(\frac{U}{R}\right)$ for each site is indicated by the circle: closed circles: $P < 0.05$; open circles: $P > 0.05$.
385 Note that the modeled results are from the pixels extracted from the same locations of the flux
386 tower sites.

387

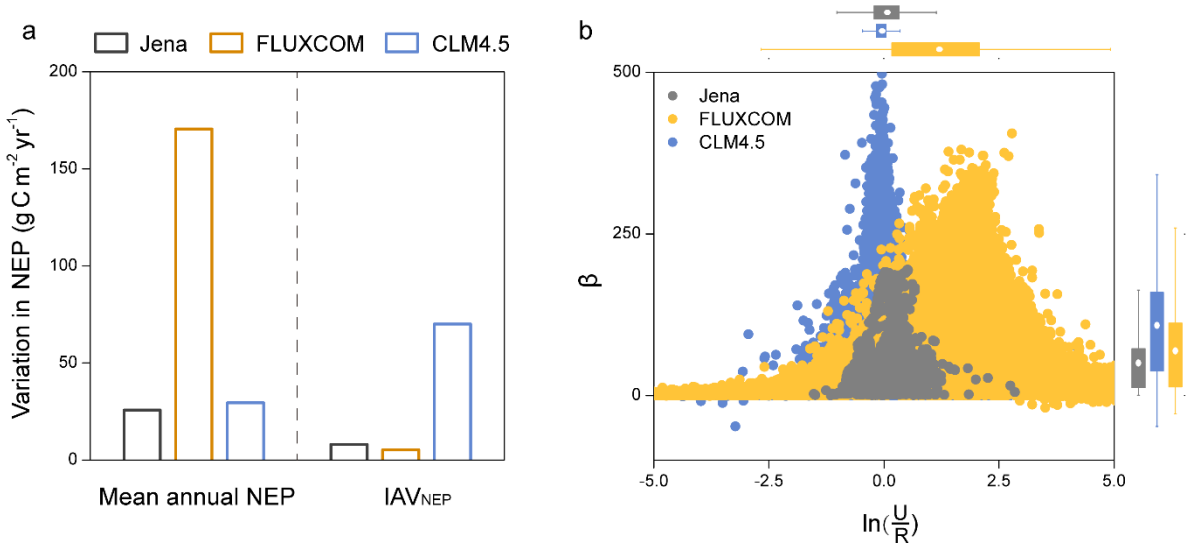

388

389 **Figure 6** Representations of the spatially varying NEP and its local indicators in FLUXCOM
390 product and the Community Land Model (CLM4.5) at the global scale. a, The variation of mean
391 annual NEP and IAV_{NEP} derives from Jena Inversion, FLUXCOM and CLM4.5. Variation in
392 mean annual NEP: the spatial variation of mean annual NEP; Variation in IAV_{NEP}: the spatial
393 variation of standard deviation in IAV_{NEP}. b, Representations of the local indicators for NEP in
394 Jena Inversion, FLUXCOM and CLM4.5.

395

References

Ahlström, A., Raupach, M. R., Schurgers, G., Smith, B., Arneth, A., Jung, M., Reichstein, M., Canadell, J. G., Friedlingstein, P., Jain, A. K., Kato, E., Poulter, B., Sitch, S., Stocker, B. D., Viovy, N., Wang, Y., Wiltshire, A., Zaehle, S., and Zeng, N.: The dominant role of semi-arid ecosystems in the trend and variability of the land CO_2 sink. Science, 348, 895-899, 2015.

Arora, V. K., Katavouta, A., Williams, R. G., Jones, C. D., Brovkin, V., Friedlingstein, P., Schwinger, J., Bopp, L., Boucher, O., Cadule, P., Chamberlain, M. A., Christian, J. R., Delire, C., Fisher, R. A., Hajima, T., Ilyina, T., Joetzjer, E., Kawamiya, M., Koven, C., Krasting, J., Law, R. M., Lawrence, D. M., Lenton, A., Lindsay, K., Pongratz, J., Raddatz, T., Séférian, R., Tachiiri, K., Tjiputra, J. F., Wiltshire, A., Wu, T., and Ziehn, T.: Carbon-concentration and carbon-climate feedbacks in CMIP6 models, and their comparison to CMIP5 models, Biogeosciences Discuss., https://doi.org/10.5194/bg-2019-473, in review, 2019.

Baldocchi, D., Chu, H., and Reichstein, M.: Inter-annual variability of net and gross ecosystem carbon fluxes: A review. Agric. For. Meteorol., 249, 520-533, 2018.

Baldocchi, D., Sturtevant, C., and Contributors, F.: Does day and night sampling reduce spurious correlation between canopy photosynthesis and ecosystem respiration? Agric. For. Meteorol., 207, 117-126, 2015.

Besnard, S., Carvalhais, N., Arain, A., Black, A., de Bruin, S., Buchmann, N., Cescatti, A., Chen, J., JClevers, J.G.P.W., Desai, A.R., Gough, C.M., Havrankova, K., Herold, M., Hörtnagl, L., Jung, M., Knohl, A., Kruijt, B., Krupkova, L., Law, B.E., Lindroth, A., Noormets, A., Roupsard, O., Steinbrecher, R., Varlagin, A., Vincke, C. and Reichstein, M.: Quantifying the effect of forest age in annual net forest carbon balance. Environ. Res. Lett., 13, 124018, 2018.

Biederman, J. A., Scott, R. L., Goulden, M. L., Vargas, R., Litvak, M. E., Kolb, T. E., Yepez, E. A., Oechel, W. C., Blanken, P. D., Bell, T. W., Garatuza-Payan, J., Maurer, . E., Dore, S., and Burns, S. P.: Terrestrial carbon balance in a drier world: the effects of water availability in southwestern North America. Glob. Change Biol., 22, 1867-1879, 2016.

Bonan, G. B., Patton, E. G., Harman, I. N., Oleson, K. W., Finnigan, J. J., Lu, Y., and Burakowski, E. A.: Modeling canopy-induced turbulence in the Earth system: a unified parameterization of turbulent exchange within plant canopies and the roughness sublayer (CLM-ml v0). Geosci. Model Dev., 11, 1467-1496, 2018.

Carpenter, S. R., and Brock, W. A.: Rising variance: a leading indicator of ecological transition. Ecol. Lett., 9, 311-318, 2006.

Churkina, G., Schimel, D., Braswell, B. H., and Xiao, X.: Spatial analysis of growing season length control over net ecosystem exchange. Glob. Change Biol., 11, 1777-1787, 2005.

Ciais, P., Tan, J., Wang, X., Roedenbeck, C., Chevallier, F., Piao, S. L., Moriarty, R., Broquet, G., Le Quéré, C., Canadell, J. G., Peng, S., Poulter, B., Liu Z., and Tans, P.: Five decades of northern land carbon uptake revealed by the interhemispheric CO_2 gradient. Nature, 568, 221-225, 2019.

Cui, E., Huang, K., Arain, M. A., Fisher, J. B., Huntzinger, D. N., Ito, A., Luo, Y., Jain, A. K., Mao, J., Michalak, A. M., Niu, S., Parazoo, N. C., Peng, C., Peng, S., Poulter, B., Ricciuto, D. M., Schaefer, K. M., Schwalm, C. R., Shi, X., Tian, H., Wang, W., Wang, J., Wei, Y., Yan, E., Yan, L., Zeng, N., Zhu, Q., & Xia, J.: Vegetation functional properties determine uncertainty of simulated ecosystem productivity: A traceability analysis in the East Asian monsoon region. Global Biogeochem. Cy., 33, 668-689, 2019.

Fu, Z., Dong, J., Zhou, Y., Stoy, P. C., and Niu, S.: Long term trend and interannual variability of land carbon uptake-the attribution and processes. Environ. Res. Lett., 12, 014018, 2017.

Fu, Z., Stoy, P. C., Poulter, B., Gerken, T., Zhang, Z., Wakbulcho, G., and Niu, S.: Maximum carbon uptake rate dominates the interannual variability of global net ecosystem exchange. Glob. Change Biol., 25, 3381-3394, 2019.

Gilmanov, T. G., Tieszen, L. L., Wylie, B. K., Flanagan, L. B., Frank, A. B., Haferkamp, M. R., Meyers, T. P., and Morgan, J. A.: Integration of CO_2 flux and remotely-sensed data for primary production and ecosystem respiration analyses in the Northern Great Plains: Potential for quantitative spatial extrapolation. Global Ecol. Biogeogr., 14, 271-292, 2005.

Gray, J. M., Frolking, S., Kort, E. A., Ray, D. K., Kucharik, C. J., Ramankutty, N., and Friedl, M. A.: Direct human influence on atmospheric CO_2 seasonality from increased cropland productivity. Nature, 515, 398-401, 2014.

Grömping, U.: Estimators of relative importance in linear regression based on variance decomposition. Am. Stat., 61, 139-147, 2007.

Huang, K., Xia, J., Wang, Y., Ahlström, A., Chen, J., Cook, R. B., Cui, E., Fang, Y., Fisher, J. B., Huntzinger, D. N., Li, Z., Michalak, A. M., Qiao, Y., Schaefer, K., Schwalm, C., Wang, J., Wei, Y., Xu, X., Yan, L., Bian C., and Luo, Y.: Enhanced peak growth of global vegetation and its key mechanisms. Nat. Ecol. Evol., 2, 1897-1905, 2018.

Jung, M., Reichstein, M., Schwalm, C. R., Huntingford, C., Sitch, S., Ahlström, A., Arneth, A., Camps-Valls, G., Ciais, P., Friedlingstein, P., Gans, F., Ichii, K., Jain, A. K., Kato, E., Papale, D., Poulter, B., Raduly, B., Rödenbeck, C., Tramontana, G., Viovy, N., Wang, Y., Weber, U., Zaehle S., and Zeng, N.: Compensatory water effects link yearly global land CO_2 sink changes to temperature. Nature, 541, 516-520, 2017.

Jung, M., Schwalm, C., Migliavacca, M., Walther, S., Camps-Valls, G., Koirala, S., Anthoni, P., Besnard, S., Bodesheim, P., Carvalhais, N., Chevallier, F., Gans, F., Goll, D. S., Haverd, V., Köhler, P., Ichii, K., Jain, A. K., Liu, J., Lombardozzi, D., Nabel, J. E. M. S., Nelson, J. A., O'Sullivan, M., Pallandt, M., Papale, D., Peters, W., Pongratz, J., Rödenbeck, C., Sitch, S., Tramontana, G., Walker, A., Weber, U., and Reichstein, M.: Scaling carbon fluxes from eddy covariance sites to globe: synthesis and evaluation of the FLUXCOM approach,

Biogeosciences, 17, 1343-1365, 2020.

Keenan, T. F., Gray, J., Friedl, M. A., Toomey, M., Bohrer, G., Hollinger, D. Y., Munger, J. W., O'Keefe, J., Schmid, H. P., Wing, I. S., Yang, B., and Richardson, A. D.: Net carbon uptake has increased through warming-induced changes in temperate forest phenology. Nat. Clim. Change, 4, 598-604, 2014.

Kunstler, G., Falster, D., Coomes, D. A., Hui, F., Kooyman, R. M., Laughlin, D. C., Poorter, L., Vanderwel, M., Vieilledent, G., Wright, S. J., Aiba, M., Baraloto, C., Caspersen, J., Cornelissen, J. H. C., Gourlet-Fleury, S., Hanewinkel, M., Herault, B., Kattge, J., Kurokawa, H., Onoda, Y., Peñuelas, J., Poorter, H., Uriarte, M., Richardson, S., Ruiz-Benito, P., Sun, I., Ståhl, G., Swenson, N. G., Thompson, J., Westerlund, B., Wirth, C., Zavala, M. A., Zeng, H., Zimmerman, J. K., Zimmermann N. E., and Westoby, M.: Plant functional traits have globally consistent effects on competition. Nature, 529, 204-207, 2016.

Le Quéré, C., Andrew, R. M., Friedlingstein, P., Sitch, S., Hauck, J., Pongratz, J., Pickers, P. A., Korsbakken, J. I., Peters, G. P., Canadell, J. G., Arneth, A., Arora, V. K., Barbero, L., Bastos, A., Bopp, L., Chevallier, F., Chini, L. P., Ciais, P., Doney, S. C., Gkritzalis, T., Goll, D. S., Harris, I., Haverd, V., Hoffman, F. M., Hoppema, M., Houghton, R. A., Hurtt, G., Ilyina, T., Jain, A. K., Johannessen, T., Jones, C. D., Kato, E., Keeling, R. F., Goldewijk, K. K., Landschützer, P., Lefèvre, N., Lienert, S., Liu, Z., Lombardozzi, D., Metzl, N., Munro, D. R., Nabel, J. E. M. S., Nakaoka, S., Neill, C., Olsen, A., Ono, T., Patra, P., Peregon, A., Peters, W., Peylin, P., Pfeil, B., Pierrot, D., Poulter, B., Rehder, G., Resplandy, L., Robertson, E., Rocher, M., Rödenbeck, C., Schuster, U., Schwinger, J., Séférian, R., Skjelvan, I., Steinhoff, T., Sutton, A., Tans, P. P., Tian, H., Tilbrook, B., Tubiello, F. N., van der Laan-Luijkx, I. T., van der Werf, G. R., Viovy, N., Walker, A. P., Wiltshire, A. J., Wright, R., Zaehle, S., and Zheng, B.: Global carbon budget 2018. Earth Syst. Sci. Data, 10, 405, 2018.

Li, G., Han, H., Du, Y., Hui, D., Xia, J., Niu, S., Li, X., and Wan, S.: Effects of warming and increased precipitation on net ecosystem productivity: a long-term manipulative experiment in a semiarid grassland. Agric. For. Meteorol., 232, 359-366, 2017.

Luo, Y., and Weng, E.: Dynamic disequilibrium of the terrestrial carbon cycle under global change. Trends Ecol. Evol., 26, 96-104, 2011.

Luo, Y., and Zhou, X.: Soil respiration and the environment. Elsevier, 2006.

Marcolla, B., Rödenbeck, C., and Cescatti, A.: Patterns and controls of inter-annual variability in the terrestrial carbon budget. Biogeosciences, 14, 3815-3829, 2017.

Musavi, T., Migliavacca, M., Reichstein, M., Kattge, J., Wirth, C., Black, T. A., Janssens, I., Knohl, A., Loustau, D., Roupsard, O., Varlagin, A., Rambal, S., Cescatti, A., Gianelle, D., Kondo, H., Tamrakar, R., and Mahecha, M. D.: Stand age and species richness dampen interannual variation of ecosystem-level photosynthetic capacity. Nat. Ecol. Evol., 1, 0048, 2017.

Niu, S., Fu, Z., Luo, Y., Stoy, P. C., Keenan, T. F., Poulter, B., Zhang, L., Piao, S., Zhou, X., Zheng, H., Han, J., Wang, Q., and Yu, G.: Interannual variability of ecosystem carbon exchange: From observation to prediction. Global Ecol. Biogeogr., 26, 1225-1237, 2017.

Novick, K. A., Oishi, A. C., Ward, E. J., Siqueira, M. B., Juang, J. Y., and Stoy, P. C.: On the difference in the net ecosystem exchange of CO_2 between deciduous and evergreen forests in the southeastern United States. Glob. Change Biol., 21, 827-842, 2015.

Oleson, K. W., Lawrence, D. M., Bonan, G. B., Drewniak, B., Huang, M., Koven, C. D., Levis, S., Li, F., Riley, W. J., Subin, Z. M., Swenson, S. C., Thornton, P. E., Bozbiyik, A., Fisher, R., Heald, C. L., Kluzek, E., Lamarque, J.-F., Lawrence, P. J., Leung, L. R., Lipscomb, W., Muszala, S., Ricciuto, D. M., Sacks, W., Sun, Y., Tang, J., and Yang, Z.-L.: Technical description of version 4.5 of the Community Land Model (CLM), NCAR Earth System Laboratory-Climate and Global Dynamics Division, Boulder, Colorado, USA, Tech. Rep. TN-503+STR, http://www.cesm.ucar.edu/models/cesm1.2/clm/CLM45_Tech_Note.pdf (last access: 27 September 2017), 2013.

Pastorello, G., Papale, D., Chu, H., Trotta, C., Agarwal, D., Canfora, E., Baldocchi, D., and Torn, M.: A new data set to keep a sharper eye on land-air exchanges. Eos, 98, 2017.

Peng, S., Ciais, P., Chevallier, F., Peylin, P., Cadule, P., Sitch, S., Piao, S., Ahlström, A., Huntingford, C., Levy, P., Li, X., Liu, Y., Lomas, M., Poulter, B., Viovy, N., Wang, T., Wang, X., Zaehle, S., Zeng, N., Zhao, F., and Zhao, H.: Benchmarking the seasonal cycle of CO_2 fluxes simulated by terrestrial ecosystem models. Global Biogeochem. Cy., 29, 46-64, 2015.

Peylin, P., Law, R. M., Gurney, K. R., Chevallier, F., Jacobson, A. R., Maki, T., Niwa, Y., Patra, P. K., Peters, W., Rayner, P. J., Rödenbeck, C., van der Laan-Luijkx, I. T., and Zhang, X.: Global atmospheric carbon budget: results from an ensemble of atmospheric CO_2 inversions. Biogeosciences, 10, 6699-6720, 2013.

Poulter, B., Frank, D., Ciais, P., Myneni, R. B., Andela, N., Bi, J., Broquet, G., Canadell, J. G., Chevallier, F., Liu, Y. Y., Running, S. W., Sitch, S., and van der Werf, G. R.: Contribution of semi-arid ecosystems to interannual variability of the global carbon cycle. Nature, 509, 600-603, 2014.

Randerson, J. T.: Climate science: Global warming and tropical carbon. Nature, 494, 319-320, 2013.

Randerson, J. T., Chapin III, F. S., Harden, J. W., Neff, J. C., and Harmon, M. E.: Net ecosystem production: a comprehensive measure of net carbon accumulation by ecosystems. Ecol. Appl., 12, 937-947, 2002.

R Development Core Team.: R: A Language and Environment for Statistical Computing 3-900051-07-0, R Foundation for Statistical Computing, Vienna, Austria, 2011.

Reichstein, M., Bahn, M., Mahecha, M. D., Kattge, J., and Baldocchi, D. D.: Linking plant and ecosystem functional biogeography. Proc. Natl Acad. Sci. USA, 111, 13697-13702, 2014.

Reichstein, M., Falge, E., Baldocchi, D., Papale, D., Aubinet, M., Berbigier, P., Bernhofer, C.,

Buchmann, N., Gilmanov, T., Granier, A., Grünwald, T., Havránková, K., Ilvesniemi, H., Janous, D., Knohl, A., Laurila, T., Lohila, A., Loustau, D., Matteucci, G., Meyers, T., Miglietta, F., Ourcival, J., Pumpanen J., Rambal, S., Rotenberg, E., Sanz, M., Tenhunen, J., Seufert, G., Vaccari, F., Vesala, T., Yakir, D., and Valentini, R.: On the separation of net ecosystem exchange into assimilation and ecosystem respiration: review and improved algorithm. Glob. Change Biol., 11, 1424-1439, 2005.

Richardson, A. D., Keenan, T. F., Migliavacca, M., Ryu, Y., Sonnentag, O., and Toomey, M.: Climate change, phenology, and phenological control of vegetation feedbacks to the climate system. Agric. For. Meteorol., 169, 156-173, 2013.

Rödenbeck, C., Zaehle, S., Keeling, R., and Heimann, M.: How does the terrestrial carbon exchange respond to inter-annual climatic variations? Biogeosciences, 15, 2481-2498, 2018.

Sakschewski, B., von Bloh, W., Boit, A., Rammig, A., Kattge, J., Poorter, L., Peñuelas, J., and Thonicke, K.: Leaf and stem economics spectra drive diversity of functional plant traits in a dynamic global vegetation model. Glob. Change Biol., 21, 2711-2725, 2015.

Scheffer, M., Bascompte, J., Brock, W. A., Brovkin, V., Carpenter, S. R., Dakos, V., Held, H., van Nes, E. H., Rietkerk, M., and Sugihara, G.: Early-warning signals for critical transitions. Nature, 461, 53-59, 2009.

Valentini, R., Matteucci, G., Dolman, A. J., Schulze, E. D., Rebmann, C. J. M. E. A. G., Moors, E. J., Granier, A., Gross, P., Jensen, N. O., Pilegaard, K., Lindroth, A., Grelle, A., Bernhofer, C., Grünwald, T., Aubinet, M., Ceulemans, R., Kowalski, A. S., Vesala, T., Rannik, Ü., Berbigier, P., Loustau, D., Guðmundsson, J., Thorgeirsson, H., Ibrom, A., Morgenstern, K., Clement, R., Moncrieff, J., Montagnani, L., Minerbi S., and Jarvis, P. G.: Respiration as the main determinant of carbon balance in European forests. Nature, 404, 861-865, 2000.

Von Buttlar, J., Zscheischler, J., Rammig, A., Sippel, S., Reichstein, M., Knohl, A., Jung, M., Menzer, O., Arain, M., Buchmann, N., Cescatti, A., Geinelle, D., Kiely, G., Law, B., Magliudo, V., Margolis, H., McCaughey, H., Merbold, L., Migliavacca, M., Montagnani, L., Oechel, W., Pavelka, M., Pelchl, M., Rambal, S., Raschi, A., Scott, R.L., Vaccari, F., Van Gorsel, E., Varlagin, A., Wohlfahrt, G., and Mahecha, M.: Impacts of droughts and extreme temperature events on gross primary production and ecosystem respiration: a systematic assessment across ecosystems and climate zones. Biogeosciences, 15, 1293-1318, 2017.

Xia, J., Chen, J., Piao, S., Ciais, P., Luo, Y., and Wan, S.: Terrestrial carbon cycle affected by non-uniform climate warming. Nat. Geosci., 7, 173-180, 2014.

Xia, J., McGuire, A. D., Lawrence, D., Burke, E., Chen, G., Chen, X., Delire, C., Koven, C., MacDougall, A., Peng, S., Rinke, A., Saito, K., Zhang, W., Alkama, R., Bohn, T. J., Ciais, P., Decharme, B., Gouttevin, I., Hajima, T., Hayes, D. J., Huang, K., Ji, D., Krinner, G., Lettenmaier, D. P., Miller, P. A., Moore, J. C., Smith, B., Sueyoshi, T., Shi, Z., Yan, L., Liang, J., Jiang, L., Zhang, Q., and Luo, Y.: Terrestrial ecosystem model performance in

simulating productivity and its vulnerability to climate change in the northern permafrost region. J. Geophys. Res-Biogeo., 122, 430-446, 2017.

Xia, J., Niu, S., Ciais, P., Janssens, I. A., Chen, J., Ammann, C., Arain, A., Blanken, P. D., Cescatti, A., Bonal, D., Buchmann, N., Curtis, P. S., Chen, S., Dong, J., Flanagan, L. B., Frankenberg, C., Georgiadis, T., Gough, C. M., Hui, D., Kiely, G., Li, J., Lund, M., Magliulo, V., Marcolla, B., Merbold, L., Montagnani, L., Moors, E. J., Olesen, J. E., Piao, S., Raschi, A., Roupsard, O., Suyker, A. E., Urbaniak, M., Vaccari, F. P., Varlagin, A., Vesala, T., Wilkinson, M., Weng, E., Wohlfahrt, G., Yan, L., and Luo, Y.: Joint control of terrestrial gross primary productivity by plant phenology and physiology. Proc. Natl Acad. Sci. USA, 112, 2788-2793, 2015.

Yu, G., Chen, Z., Piao, S., Peng, C., Ciais, P., Wang, Q., Li, X., and Zhu, X.: High carbon dioxide uptake by subtropical forest ecosystems in the East Asian monsoon region. Proc. Natl Acad. Sci. USA, 111, 4910-4915, 2014.

Zeng, N., Zhao, F., Collatz, G. J., Kalnay, E., Salawitch, R. J., West, T. O., and Guanter, L.: Agricultural Green Revolution as a driver of increasing atmospheric CO_2 seasonal amplitude. Nature, 515, 394-397, 2014.

Zhao, J., Peichl, M., Öquist, M., and Nilsson, M. B.: Gross primary production controls the subsequent winter CO_2 exchange in a boreal peatland. Glob. Change Biol., 22, 4028-4037, 2016.

Zhou, S., Zhang, Y., Ciais, P., Xiao, X., Luo, Y., Caylor, K. K., Huang, Y., and Wang, G.: Dominant role of plant physiology in trend and variability of gross primary productivity in North America. Sci. Rep., 7, 41366, 2017.